Article

pubs.acs.org/Biomac

Importance of Sequence Specific Hydrophobicity in Synthetic Protein Transduction Domain Mimics

Federica Sgolastra,[†] Lisa M. Minter,[‡] Barbara A. Osborne,[‡] and Gregory N. Tew*[,†,‡]

Departments of [†]Polymer Science and Engineering and [‡]Veterinary and Animal Sciences, University of Massachusetts, Amherst, Massachusetts 01003, United States

Supporting Information

ABSTRACT: A new series of synthetic protein transduction domain mimics (PTDMs) was designed to analyze the importance of guanidine and phenyl group segregation along the backbone on their membrane interaction and cellular internalization abilities. ROMP was utilized to synthesize three polymers: nonsegregated homopolymers, intermediately segregated gradient copolymers, and strongly segregated block copolymers. In order to understand the role of functional group segregation on activity, it was important to design monomers that enabled these three different polymer topologies, or constitutional macromolecular isomers, to be prepared with identical chemical compositions. The structure–activity relationships were evaluated by both a biophysical assay, using dye-loaded vesicles, and by in vitro cellular uptake studies of fluorescently labeled chains. The results showed that functional group segregation impacts activity. In general, the nonsegregated homopolymer was the most active in both assays but also showed larger, ill-defined aggregates compared to either the gradient or block copolymers. It was also the most cytotoxic of the three isomers. As a result, the gradient copolymer with intermediate segregation optimizes activity and solubility with low cytotoxicity. This study gives new design guidelines for the development of PTDMs.

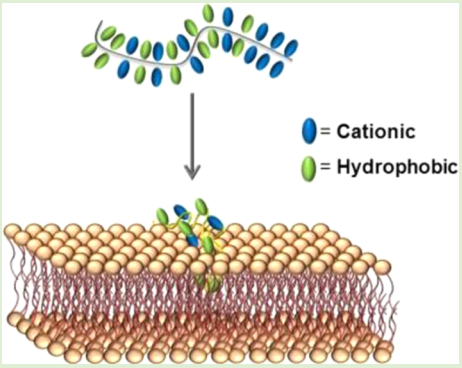

INTRODUCTION

Protein transduction domains (PTDs), a class of cell penetrating peptides (CPPs), are short cationic protein segments with the ability to traverse the phospholipid bilayer and accumulate inside cells.[1] The first protein discovered with these properties was the TAT protein from HIV-1.[2,3] Following studies found that TAT's translocation capability was due to the basic domain between residues 48–60[4] and largely attributed to the presence of arginine residues. Guanidinium groups have since been shown to interact with the negative components of the cell surface facilitating translocation,[5,6] although the exact mechanism of cellular uptake is still under debate.[7] Many mechanisms have been proposed, although they are typically classified as either energy-independent or energy-dependent.[8] It is believed that most CPPs utilize a combination of both mechanisms. Energy-independent pathways may include inverted micelle formation, pore formation, carpet-like model, and the membrane-thinning model. Energy-dependent pathways instead include different types of endocytosis.

Since the first discovery of TAT, a large number of highly charged, cationic PTDs have been reported, including penetratin,[9] pVEC,[10] VP22,[11] polyarginines,[12] and transportan.[13] Some of these PTDs contain a hydrophobic component, which has been suggested to improve their membrane transduction activity. Consistent with this hypothesis, N-terminal stearylation/acylation of polyarginine,[14,15] as well as the addition of supramolecular hydrophobic counterions,[16−18] have been shown to improve both membrane affinity and cellular internalization. Aromaticity has also been shown to play a role in membrane interaction and translocation.[19−21] For example, the activity of oligoarginine was enhanced when aromatic as opposed to aliphatic counterions were added or when tryptophan and phenylalanine were included in the peptide sequence.[22−25]

We previously reported the synthesis and preliminary investigations of oxanorbornene-based guanidine rich polymer mimics of polyarginine, which showed higher membrane activity than in the polyarginine counterparts. This was evaluated by both their ability to release dye from large unilamellar vesicles (LUV)[26] and by cellular internalization into various cell types (HEK 293T, CHO, Jurkat).[27] One of the advantages offered by the synthesis of polymeric mimics over peptide derivatives of PTDs is their functional and structural versatility. For example, our chemical platform allows for the tuning of the overall hydrophobic content by incorporating different alkyl as well as aromatic side chains.[28,29] As already observed for polyarginine derivatives, the incorporation of hydrophobic residues further increased the membrane activity of these PTDMs. It was also easy to increase guanidium density

Received: November 5, 2013
Revised: February 7, 2014
Published: February 10, 2014

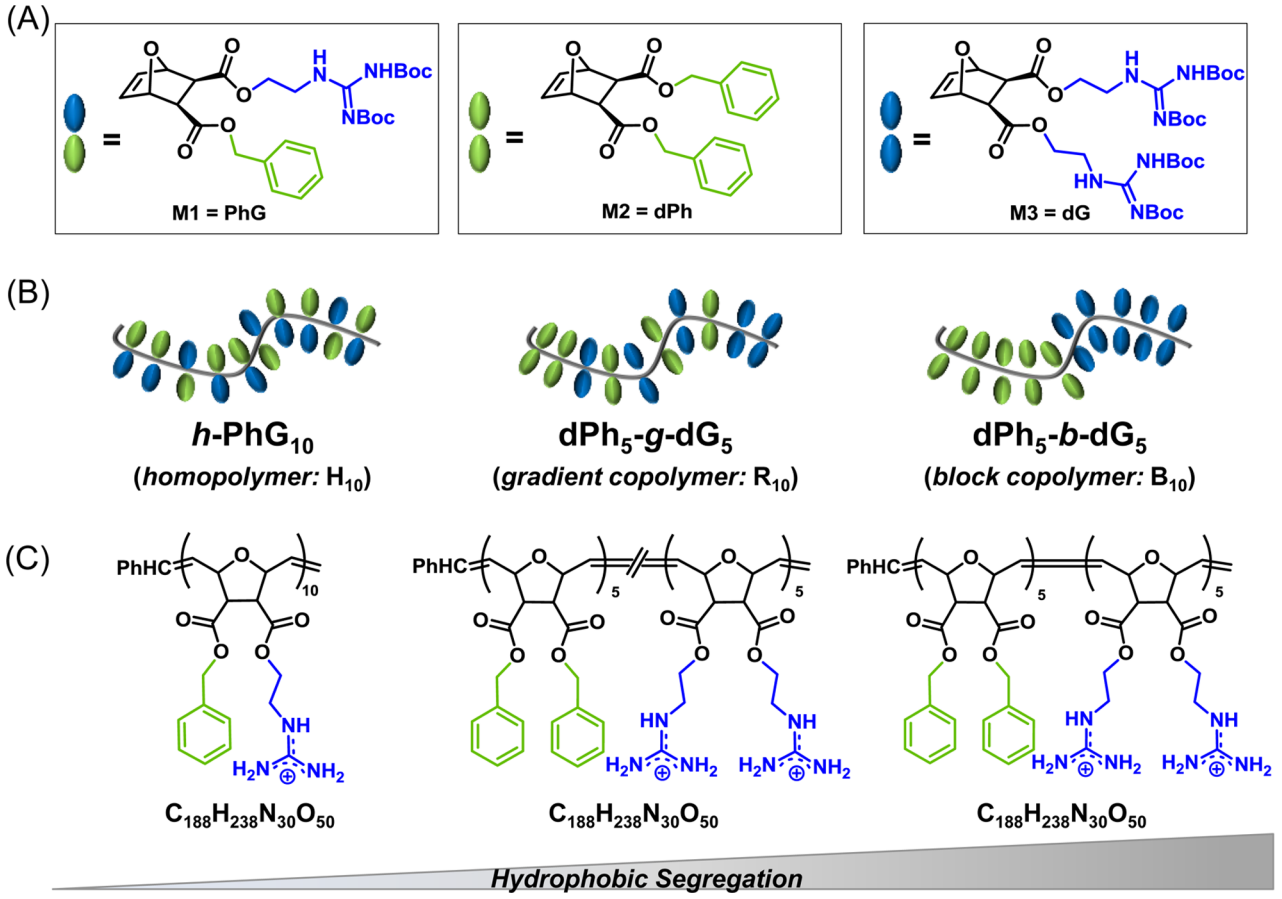

Figure 1. Structures of monomers and related constitutional macromolecular isomers used in this study. (A) Chemical structures of monomers, (B) representative cartoons of the polymeric isomers, and (C) corresponding polymer chemical structures with their average chemical formulas, counterions omitted for clarity. Green and blue represent the hydrophobic and the cationic components, respectively.

along the backbone, which significantly increased cellular uptake.[27]

Several model peptides have been prepared in an effort to study the role of hydrophobicity on uptake; however, because these peptides also adopt secondary structures, it has proven difficult to decouple the influence of sequence specific hydrophobicity (i.e., identical side chain composition but different arrangement within the backbone) on activity due to the folded structure. Of the model peptides that have been reported, there are primary amphiphilic, block copolymer-like structures, such as Pep-1[30] and pVEC,[10] as well as secondary amphipathic helices like MAP.[31,32] Some studies indicate that the block copolymers are more membrane active than the facially amphiphilic helix.[33] Moreover, the cellular uptake of pVEC was significantly higher than the nonamphipathic scrambled-pVEC, in which the N-terminal hydrophobic residues of the original sequence were randomly placed within the cationic domain.[34] In another example, uptake studies performed on a series of MAP derivatives using HPLC had initially established that amphiphilicity was crucial for internalization;[35] however, following investigations using confocal laser scanning microscopy did not show any substantial differences in the membrane crossing efficiencies of amphiphilic over nonamphiphilic peptides.[36] As a result, the role of amphiphilicity on activity remains unclear but is an important area of design to increase potency. Among synthetic, nonpeptidic PTDMs, no reports can be found that adequately addresses the importance of sequence specific hydrophobicity on their membrane activity, despite the recent expansion of PTDM chemistry that includes both new homopolymers and block copolymers.[37−42]

Our synthetic approach to PTDMs allowed us to determine if, and how, the activity of polymeric PTDMs varies as a function of the spatial arrangement of the positive charges and the hydrophobic groups. We developed a series of homologous PTDMs in which the guanidine and hydrophobic groups were either in the same or in separate repeat units, generating homopolymers, gradient copolymers, and block copolymers with the same chemical composition but increasing segregation (Figure 1). Given the identical chemical composition of these three polymers but the important differences with respect to the arrangement of the functional group side chains, a more descriptive terminology would be helpful. Although "sequence isomerism" is a term previously used in the polymer literature, this specifically refers to a head-to-tail orientation, typical of vinyl monomers like propylene.[43] It has also been used in the peptide community to mean identical side chain composition but a different arrangement within the backbone.[44] To avoid any confusion, we prefer "constitutional macromolecular isomerism" because all three isomers have identical elemental formulas yet different arrangements of the guanidine and aromatic groups along the backbone.

The capability and efficiency of these constitutional macromolecular isomers to act as PTDMs were measured in two different assays: a biophysical experiment based on dye release from vesicles for evaluating membrane perturbation capabilities,

dx.doi.org/10.1021/bm401634r | Biomacromolecules 2014, 15, 812−820

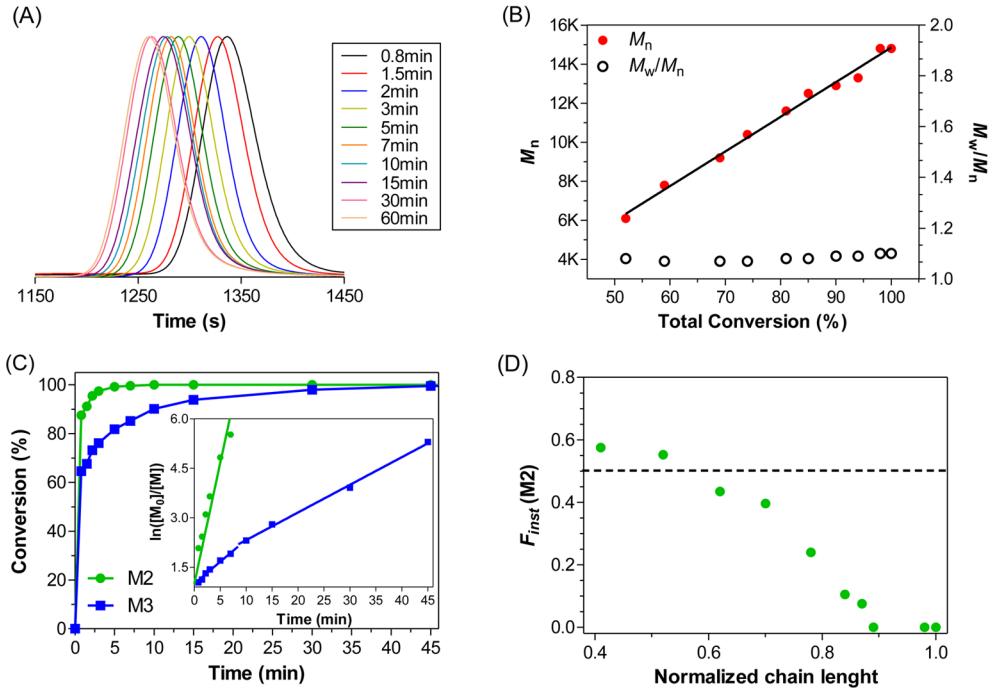

Figure 2. ROMP kinetic studies for the random copolymerization of M2 (diphenyl) and M3 (diguanidine) monomers in CH_2Cl_2 at room temperature. (A) GPC traces of the polymer at each time point recorded using an RI detector and THF as the eluent. (B) Polymer M_n and M_w/M_n (PDI), as calculated from GPC using polystyrene standards vs total monomer conversion (from ^{1}H NMR). (C) Conversion of M2 (green) and M3 (blue) as a function of time as calculated from ^{1}H NMR. (Inset) Linear fits of the first-order time-conversions of M2 (green) and M3 (blue). (D) F_{inst} of M2 vs normalized chain length. The dotted line represents the expected F_{inst} plot for a random, gradient-free copolymerization. $[M2]_0 = [M3]_0 = 0.066$ M, $[M2 + M3]_0/[G3]_0 = 40/1$.

and a biological, in vitro assay for the cellular uptake of dye-labeled derivatives at different physiological conditions. In general, we found that hydrophobic segregation does play a role in PTDM activity, especially at high concentrations. An increase in functional group segregation led to a decrease in activity, since the block copolymer performed less efficiently compared to the other isomers, probably because of its tendency in aqueous environments to form micelles in which the hydrophobic domain is hidden in the core, thus, unavailable to interact with the membrane.

EXPERIMENTAL SECTION

PTDM Synthesis. The detailed synthetic procedures are reported in the Supporting Information (Schemes S1 and S2). Briefly, the product of Diels–Alder reaction between maleic anhydride and furan was ring-opened with the desired alcohol to introduce the first side chain. A second side chain was then introduced by EDC coupling with one equivalent of the required alcohol. The desired polymers were obtained by ROMP using the Grubbs' third generation catalyst (G3)[45] in dichloromethane (CH_2Cl_2), with polydispersity indices under 1.1 (PDIs = M_w/M_n). To simplify the polymerization conditions, guanidine groups in the monomers were Boc-protected, and the Boc groups were removed after polymerization by treatment with trifluoroacetic acid. The final products were purified by dialysis against RO water and recovered by lyophilization.

Preparation of EYPC-LUVs⊃CF. A thin lipid film was prepared by evaporating a solution of 25 mg EYPC in chloroform on a rotary evaporator (room temperature) and then in vacuum overnight protected from light. After hydration (~1 h) with 1.0 mL of buffer A (10 mM Tris, 10 mM NaCl, 50 mM CF, pH 7.5) accompanied by occasional vortex, the resulting suspension was subjected to six freeze–thaw cycles (liquid N_2 to freeze and 25 °C water bath to thaw), and then extruded 11 times through a polycarbonate membrane (pore size 100 nm). Extravesicular dye was removed by size exclusion chromatography (Sephadex G-50 superfine, Sigma-Aldrich) with Tris saline buffer (10 mM Tris, 107 mM NaCl, pH 7.5).

Dye Release Experiment. All fluorescence measurements were taken at 25 °C with an excitation frequency of 492 nm and an emission of 517 nm. After measuring the baseline fluorescence of a fixed amount of EYPC-LUVs⊃CF, increasing concentrations of PTDMs were added while stirring. After 10 min of shaking the fluorescence intensity was measured again. Results were normalized according to the baseline and the total fluorescence (measured after the addition of Triton X-100 to release all dye from the vesicles) to yield fractional dye release Y (see Supporting Information for details).

Cell Culture. Jurkat-T cells (human T lymphocyte leukemia cell line) and HEK293T cells (human embryonic kidney 293 cell line) were grown in RPMI 1640 and DMEM, respectively, supplemented with 10% (v/v) FBS, glutamine, 100 U/mL penicillin, and 100 U/mL streptomycin. Jurkat-T cells were incubated at 37 °C with 5% CO_2 and passaged the day before the treatment. On the day of the experiment, NBD-labeled PTDM solutions in PBS were added to 1×10^6 cells in 1 mL of complete cell growth medium. HEK293T cells were plated the day before the treatment (4×10^5 cells/mL in a 12-well plate) in order to be about 80% confluent on the day of the experiment. Cells were incubated with the polymers at 37 °C for 30 min, then analyzed by flow cytometry (see Supporting Information for detailed procedure).

RESULTS AND DISCUSSION

PTDM Design Principles and Characterization. We developed a series of constitutional macromolecular isomers in which the functional group arrangement along the backbone was the only variable element. It was specifically important to keep the molecular weight and the ratio of hydrophobic-to-cationic side chains constant, since both of these features can influence activity.[26,28,46] For this purpose, we utilized the "molecular construction kit" previously developed in our laboratory[47] that allows independent variation of the two side

dx.doi.org/10.1021/bm401634r | Biomacromolecules 2014, 15, 812–820

chains in each monomer. These difunctional monomers can be efficiently polymerized by ring-opening metathesis polymerization (ROMP) into polymers with well-defined architectures (Figure 1A). ROMP is a powerful method for the efficient and rapid synthesis of novel macromolecules with well-defined structures, as it has a high functional group tolerance and allows control over molecular weight and polydispersity. Being a living polymerization, it also generates less heterogeneity among polymer chains than, for example, traditional free radical methods when two or more monomers are copolymerized. The choice of a phenyl group (Figure 1A) as the hydrophobic side chain stems from previous studies on the role of aromaticity with respect to membrane activity.[19,29]

We therefore designed and synthesized three constitutional macromolecular isomers with increasing hydrophobic segregation: a homopolymer, *h*-PhG_{10}, in which the cationic and hydrophobic side chains are both present in every repeat unit and thus homogenously distributed along the chain; a gradient copolymer, dPh_5-*g*-dG_5, where the two functionalities reside on different repeat units but as a result of the polymerization conditions are only partially segregated; and finally a block copolymer, dPh_5-*b*-dG_5, in which the two functionalities are completely segregated along the backbone, thus, mimicking the primary amphiphilic topology of many peptidic PTDs (Figure 1B,C).

The homopolymer *h*-PhG_{10} was synthesized in 45 min from monomer M1 using a monomer-to-catalyst ratio of 10 to 1. Monomers M2 and M3 were polymerized together as a 1:1 mixture to give the gradient copolymer dPh_5-*g*-dG_5. The block copolymer dPh_5-*b*-dG_5 was obtained instead by the stepwise polymerization of each block. First the hydrophobic block was synthesized from monomer M2, then, after 10 min, monomer M3 was added to form the guanidine-containing block. The diblock copolymer topology was confirmed by gel permeation chromatography (GPC, see Figure S1, Supporting Information). The GPC traces showed a shift of the final diblock (red curve) toward higher molecular weight compared to the first block (blue curve), with no evidence of unreacted first block left at the end of the polymerization. Moreover, the conservation of a monomodal and narrow distribution throughout the process indicated efficient chain extension. All the polymers in the series showed similar molecular weights with narrow PDIs (<1.1), as determined by GPC (Figure S2, Supporting Information), and a phenyl-to-guanidine ratio of 1:1, as determined via ^{1}H NMR spectroscopy.

The topology of the gradient copolymer was confirmed by polymerization kinetics. Figure 2 shows the results for a typical kinetic analysis of ROMP for a M2/M3 (1:1) mixture, where the molar ratio of M2 + M3 to G3 was 40:1 and the initial monomer concentration was fixed at 0.066 M in CH_2Cl_2, same as for the dPh_5-*g*-dG_5 synthesis. Given the rate of the polymerization, we increased the monomer-to-catalyst ratio to facilitate data collection over a reasonable time period. GPC analyses showed a constant increase of molecular weight over time, with a symmetrical and monomodal molecular weight distribution at each time point, and a linear increase of M_n over total monomer conversion as determined by ^{1}H NMR spectroscopy (Figure 2A and B, respectively). The PDI remained under 1.1 throughout the polymerization. These data support the controlled ROMP of M2 and M3.

However, looking at the individual monomer conversions over time, they show different conversion rates: M2 reached 100% conversion in less than 10 min, while M3 required 45 min (Figure 2C). The different polymerization behavior of the two monomers can be even better appreciated in the semilogarithmic plot of monomer concentration versus time (Figure 2C, inset) obtained from the conversion percentages at each time point. While the two curves were approximately linear, indicating first-order kinetics for both monomers typical of a living polymerization, their polymerization rate constants (k_p) derived from the plot slopes were very different. M2 had a faster k_p of $(12.19 \pm 0.85) \times 10^{-3}$ L /(mol·s), indicating faster incorporation, while M3 had a slower polymerization rate with two regimes: an initial k_p of $(2.22 \pm 0.09) \times 10^{-3}$ L/(mol·s) and then an even slower one of $(1.40 \pm 0.05) \times 10^{-3}$ L/(mol·s) once M2 has been completely consumed.[48] From the monomer conversion data, instantaneous composition (F_{inst})[49] was also calculated (Figures 2D and S3) and appeared to deviate from what is normally expected for a random copolymerization (dotted line). These data suggest that the copolymer obtained is not random but rather is better described as a gradient topology, with a relatively small change in instantaneous monomer composition.[50] As Figure 2D shows, when a chain is 40 monomers long, there are on average four M3 monomers (diguanidine) at the end of the chain. For the DP = 10 isomers studied in detail, this translates to one M3 at the chain end on average.

Polymer Aggregation. Because the different self-assembly and aggregation properties dictated by the various polymer architectures may be a key factor in determining lipid membrane interactions, we characterized the PTDMs' aggregation profiles in aqueous solution. Dynamic light scattering (DLS) measurements suggested that the homopolymer formed aggregates with a diameter of ~140 nm, while both the gradient and the block copolymers formed smaller assemblies of similar size (~18 nm), correlating with a micelle-like structure with a hydrophobic core and a cationic shell (Table 1). One outcome of the different copolymer architecture would be that the micellar assembly of the gradient copolymer, dPh_5-*g*-dG_5, with a shorter corona, exposes more of the hydrophobic groups to the external environment, leading to increased interactions with lipid membranes. This is consistent with previous studies showing that the primary polymer sequence impacted micelle formation.[51,52]

Table 1. Size and Zeta Potential of Polymers (4 μM) in Tris Buffer (pH = 7.5)[a]

sample size	(d·nm)	zeta (mV)
h-PhG_{10}	138 ± 10	+18 ± 3
dPh_5-*g*-dG_5	18 ± 5	+27 ± 5
dPh_5-*b*-dG_5	17 ± 3	+31 ± 7

[a]Mean ± standard deviation (S.D.) of three independent measurements.

Zeta potential measurements showed that all particles were positively charged, as expected because of the guanidine-containing residues. The homopolymer had a lower zeta potential value (+18) compared to the gradient and block copolymers (~+30), probably due to the lower surface exposure of the cationic groups in the aggregate compared to the micelles, where they are preferentially localized in the corona.

Vesicle Assay. For a PTD(M) to access the cytosol, it must cross either the plasma membrane, or the endosomal membrane if internalized by endocytosis. Therefore, the effect

dx.doi.org/10.1021/bm401634r | Biomacromolecules 2014, 15, 812−820

of the sequence specific hydrophobicity on membrane activity was first evaluated with a standard biophysical assay. One method to measure membrane activity is a liposomal dye release assay[53] in which carboxyfluorescein (CF) is encapsulated inside liposomes at a high concentration where its intrinsic fluorescence is quenched. If increasing PTDM concentration causes CF release, which is measured as an increase in fluorescence, this has been related to membrane activity (see Supporting Information for detailed procedures).[22,26,28,29,54,55] In the specific case studied here, LUVs composed of egg yolk phosphatidylcholine (EYPC) were used as a model for the mammalian plasma membrane. As shown in Figure 3A, for each PTDM isomer tested, the membrane activity, reported as fractional fluorescence intensity (Y), increased with increasing polymer concentration in a nonlinear fashion until it reached a plateau. Fitting the Hill equation (equation S2, Supporting Information) to these data, yielded the maximum activity, Y_{max} (i.e., the total amount of dye released at high PTDM concentration), and the EC_{50}, the effective concentration at which each PTDM shows 50% of its total activity ($Y_{max}/2$; Figure 3B).

While all three PTDM isomers showed similar EC_{50} values ($\sim 2 \times 10^{-8}$ M), they differed significantly in their Y_{max}. The activity of the homopolymer *h*-PhG_{10} was nearly twice that of the block copolymer dPh_5-*b*-dG_5 (88% of maximum dye release instead of 46%), while the gradient copolymer dPh_5-*g*-dG_5 showed intermediate activity (71%) closer to the homopolymer. This suggested that the homopolymer, with the side chains evenly distributed along the backbone, was more active than the gradient and block copolymers. In turn, the gradient copolymer was more active than the block copolymer. The same trend was maintained but was even more prominent at higher molecular weight, as seen for a series of polymers with DP = 20 (Figure S5, Supporting Information). Although the Y_{max} values for the DP = 20 series were similar to the DP = 10 series, the EC_{50} values began to diverge. Again, the homopolymer was the most active of the three constitutional macromolecular isomers ($EC_{50} = 0.7 \times 10^{-8}$ M and Y_{max} = 86%) followed by the gradient copolymer ($EC_{50} = 1 \times 10^{-8}$ M and Y_{max} = 71%) and then the block copolymer ($EC_{50} = 2 \times 10^{-8}$ M and Y_{max} = 45%). The same trend was also observed within the series containing different hydrophobic, nonaromatic groups (cyclohexyl) as side chains (data not shown), confirming that it is indeed a sequence specific hydrophobicity effect exclusively.

This simple biophysical assay shows that the dye release activity decreases with increasing hydrophobic segregation. The homopolymer, which has a nonsegregated design, is more membrane active than the most strongly segregated block copolymer, whereas the gradient copolymer showed an intermediate behavior but closer to the homopolymer than block copolymer. This trend could be attributed to the different degrees of hydrophobic side chain exposure at the surface of the polymer aggregates (higher in the homopolymer, lowest in the block copolymer), due to the different self-assembly behavior in aqueous environments described in the previous section. In the less-active block copolymer, the hydrophobic residues are packed in the micelle core, which prevents them from interacting with the lipid membrane. These results are in accordance with those recently reported by Aoshima and Kuroda,[56] in which amphiphilic block copolymers did not induce dye release from mammalian-like lipid vesicles, while less ordered random copolymers were able to efficiently interact with this type of membrane.

Cellular Uptake Assays. The ability of different constitutional macromolecular isomeric PTDMs to be internalized into cells was first evaluated with Jurkat-T cells.[37] Although vesicle studies suggested improved activity and a higher influence of hydrophobic segregation for the DP = 20 series, we chose to use the DP = 10 series for the in vitro studies to limit cytotoxicity side effects.[27,57] To determine the appropriate conditions for the cellular treatment, viability profiles for the three PTDM isomers were measured via both MTT and 7-AAD assays over a range of concentrations. The MTT assay was used to judge whether the treatment influences the metabolic activity of the cells, as assessed by their ability to enzymatically convert the tetrazolium dye MTT into formazan.[58] On the other hand, the 7-AAD assay was used to assess cellular membrane integrity after treatment.[59] As shown in Figure 4, both assays gave similar results. Starting at a

(A)

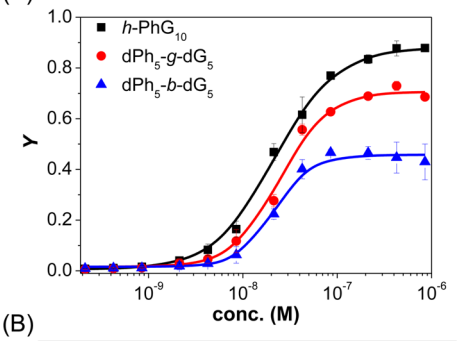

(B)

Sample	EC_{50} (nM)[a]	Y_{max} (%)[b]
h-PhG_{10}	22.0 ± 3.1	88 ± 1
dPh_5-*g*-dG_5	24.9 ± 0.6	71 ± 1
dPh_5-*b*-dG_5	22.0 ± 1.6	46 ± 4.5

Figure 3. PTDM-induced dye release from CF-loaded EYPC-vesicles. (A) Fractional membrane activity (Y) vs polymer concentration with Hill equation fit; (B) EC_{50} and Y_{max} values for each constitutional macromolecular isomer (degree of polymerization, DP = 10). [a]EC_{50}: effective polymer concentration needed to reach $Y_{max}/2$; [b]Y_{max}: maximal fractional CF release relative to the total release obtained by Triton X-100. Each data point represents the mean ± SD from three independent measurements.

polymer concentration of 8 μM, a decrease in viability was observed by both assays when treated with the homopolymer, *h*-PhG_{10}. The production of formazan was reduced to about 60% compared to the control and about 30% of cells stained positive for 7-AAD. In contrast, the gradient copolymer and the block copolymer, dPh_5-*g*-dG_5 and dPh_5-*b*-dG_5, did not show significant toxicity even at higher concentrations. To avoid any potential toxicity in the following uptake experiments, cells were treated with either 2 or 4 μM of each polymer for 30 min in RPMI media containing 10% fetal bovine serum.

Cellular uptake of each PTDM in Jurkat-T cells was quantified using flow cytometry. In order to use this method, the PTDMs tested were fluorescently labeled. While choosing the fluorescent reporter to add, it is important to consider that the charge as well as the hydrophobicity of the fluorophore can affect the cellular uptake and distribution of the attached PTDM, as has been shown for the negatively charged and commonly used fluorescein (FITC)[60−62] as well as the

dx.doi.org/10.1021/bm401634r | *Biomacromolecules* 2014, 15, 812−820

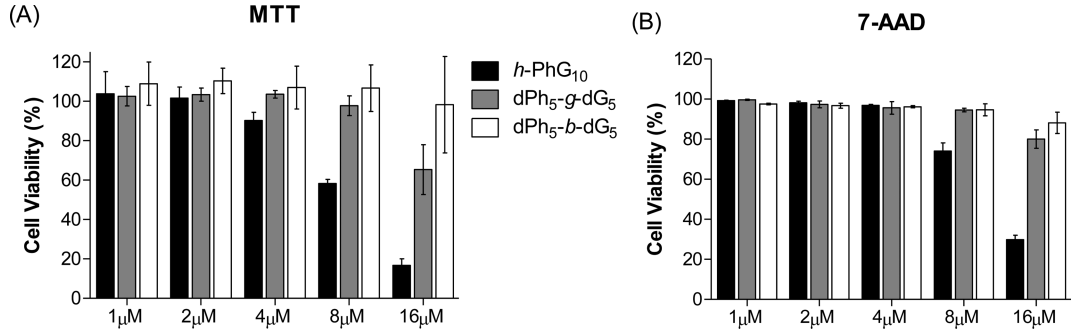

Figure 4. Cell viability as measured by (A) MTT and (B) 7-AAD assay. Jurkat-T cells (1×10^6cells/mL) were treated for 30 min with increasing concentration of polymers in complete growth media at 37 °C before performing the specific viability assays.

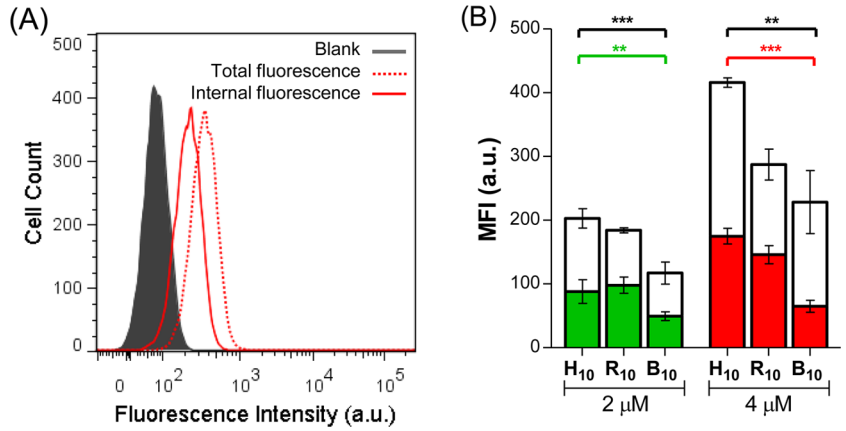

Figure 5. Jurkat-T cell uptake according to NBD/dithionite assay. (A) Representative histograms obtained from flow cytometric analysis showing the cellular uptake of 4 μM NBD-labeled dPh_5-*g*-dG_5 (R_{10}) at 37 °C in complete growth media. The solid black curve represents untreated Jurkat-T cells; the dotted and solid red lines represent cells treated with the polymer before and after treatment with 1 mM dithionite solution, respectively. (B) Jurkat-T cells treated with 2 (green) or 4 μM (red) of NBD-labeled polymer (H_{10}: NBD-*h*-PhG_{10}; R_{10}: NBD-dPh_5-*g*-dG_5; B_{10}: NBD-dPh_5-*b*-dG_5) in complete growth media at 37 °C for 30 min. White open bars represent the amount of membrane-bound polymers, while solid colored bars represent the amount of polymer internalized, as measured by the NBD/dithionite assay. MFI: mean fluorescence intensity relative to untreated samples. Each point represents the mean ± SD of three independent experiments; $^{**}p < 0.01$, $^{***}p < 0.001$ of H_{10} vs B_{10} (total or internalized), as calculated by repeated-measures one-way ANOVA with Tukey posthoc test.

zwitterionic carboxyrhodamine (TAMRA).[63] Additionally, the position of the fluorescent reporter within the transduction moiety can also alter the activity of the transporter.[64] In order to limit the physicochemical alteration of our system, we chose the small (139 Da), neutral 7-nitrobenz-2-oxo-1,3-diazol-4-yl (NBD)[65] as the fluorescent reporter for this study, which was covalently attached at one end of the polymer chain. For the synthesis of the end-labeled PTDMs, polymers end-capped with a succinimide-functionalized ester monomer were synthesized, and then the activated ester was exchanged with an ethylenediamine-functionalized NBD dye, resulting in the NBD-labeled homopolymer H_{10}, gradient copolymer R_{10}, and block copolymer B_{10} (Supporting Information for detailed synthesis).[27] We termed the gradient copolymer R_{10} since the use of G_{10} could be confused with the guanidine-containing monomers used in the more descriptive polymer names like *h*-PhG_{10}; it also highlights another point, which is that when gradient polymers have small DPs, they are also similar to random copolymers. The successful incorporation of the dye into the polymers was determined using UV−vis spectroscopy and UV-capable GPC (Figure S4, Supporting Information).

The use of NBD as the fluorescent label also allowed us to differentiate between membrane-bound and internalized PTDMs. Since NBD is irreversibly quenched by brief exposure to the membrane impermeable reducing agent dithionite ($S_2O_4^{2-}$), a washing step with a basic solution of sodium dithionite depletes the fluorescence from surface-bound molecules exclusively, allowing for measurement of the fluorescence only from internalized molecules.[66,67]

Figure 5A shows a representative fluorescent cell distribution analysis in an NBD/dithionite assay as measured via flow cytometry. The dotted red curve represents the total fluorescence from both internalized and surface-bound molecules. After dithionite quenching, the histogram (solid red curve) shifted to lower fluorescence intensity values corresponding to only internalized molecules. The mean fluorescence intensity (MFI) of the cellular fluorescence distribution after dithionite quenching was used as a measure of polymer internalization efficacy, while the difference between the MFIs before and after the quenching represented the amount of polymer that was bound to the membrane but not internalized. Figure 5B shows the impact of sequence specific hydrophobicity on the cell-surface binding (difference between the fluorescence measured before and after dithionite treatment, open bars) and cell internalization efficiencies (following dithionite quenching, solid bars) at the two polymer concentrations tested.

For each PTDM isomer tested, the total amount of cell-associated molecules (membrane-bound plus internalized) increased with increasing concentration. For example, when

dx.doi.org/10.1021/bm401634r | *Biomacromolecules* 2014, 15, 812−820

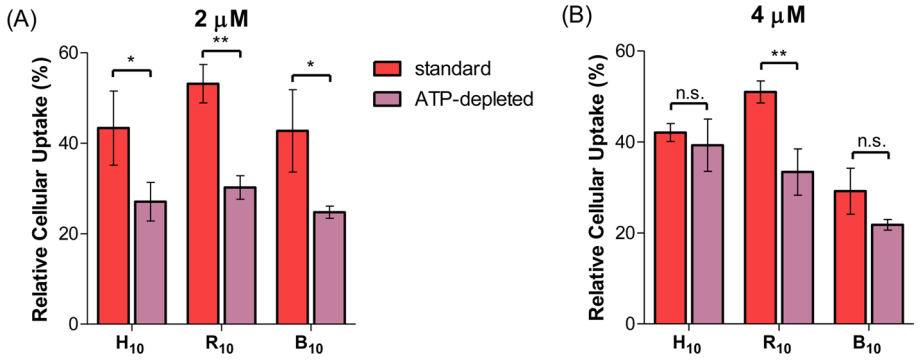

Figure 6. Internalization under energy-depleted conditions. Jurkat-T cells were incubated for 30 min with 2 or 4 μM of NBD-labeled polymer (H_{10}: NBD-*h*-PhG_{10}; R_{10}: NBD-dPh_5-*g*-dG_5; B_{10}: NBD-dPh_5-*b*-dG_5) at standard conditions (red bars) or after cellular ATP depletion (purple bars). For depletion of cellular ATP, cells were preincubated for 30 min with 10 mM sodium azide and 25 mM of 2-deoxy-D-glucose.[77] Relative cellular uptake values are calculated as the percentage ratio between internal and total fluorescence (in MFI). Each point represents the mean ± SD of three independent experiments; $*p < 0.05$, $**p < 0.01$, n.s. $p > 0.05$, as calculated by unpaired two-tailed student *t*-test.

cells were treated with 4 μM instead of 2 μM of either H_{10} or B_{10}, the resultant MFI values essentially doubled (416 ± 13 instead of 203 ± 6 for H_{10} and 228 ± 57 instead of 117 ± 11 for B_{10}). Although more evident for the 4 μM treatment than the 2 μM one, both the homopolymer H_{10} and the gradient copolymer R_{10} performed significantly better than the block copolymer B_{10}. For example, in the 4 μM treatment, the MFI relative to the amount of PTDM internalized by the cells was 146 ± 14 for R_{10} versus 65 ± 10 for B_{10}. Because of its lower cytotoxicity, the gradient copolymer R_{10} is preferred to the homopolymer H_{10} for biological applications.

The relative internalization efficiencies of the NBD-labeled PTDMs were also evaluated in terms of relative percent cellular uptake with respect to the total cell-associated MFI (see Figure S6, Supporting Information), which indicates the equilibrium ratio between cell surface-bound PTDMs and internalized PTDMs. At a polymer concentration of 4 μM, the cellular uptake of both H_{10} and R_{10} (42 ± 2% and 51 ± 2%, respectively) were again significantly higher than B_{10} (29 ± 5%) and R_{10} was the most efficient of all three isomers.

In order to determine if the observed trend was cell-specific, we also measured PTDM internalization efficiency in HEK293T, an adherent cell-type (Figure S7, Supporting Information). When comparing the MFI from internalized PTDMs (solid colored bars), a similar trend to that observed in Jurkats was seen. H_{10} and R_{10} showed the same activity and both were internalized more efficiently than B_{10}. This suggests that, besides some expected cell-type variability, the overall major trend observed is not cell-type specific.

Taken together, these biological data indicate that strong hydrophobic segregation has a negative impact on both the membrane binding process (the equilibrium between PTDMs in solution and cell surface-bound PTDMs, represented by the total MFI) and the internalization process (the equilibrium between PTDMs on the surface and inside the cells, represented by the relative percent cellular uptake), since these processes decreased going from the nonsegregated homopolymer to the fully segregated block copolymer.

In an effort to differentiate between energy-dependent and energy-independent internalization pathways, we performed the cellular uptake assay in ATP-depleting conditions known to inhibit endocytosis.[68] Figure 6 shows the relative percentage of cellular uptake[27] when Jurkat-T cells were incubated at 37 °C either in standard complete growth medium or in glucose-free medium supplemented with 2-deoxyglucose/sodium azide (ATP-depleting medium, see Figure S8 in Supporting Information for the raw data in MFI). At 2 μM concentration, we observed a basal-level, ATP-sensitive contribution to the cellular uptake for each of the PTDMs. In the presence of ATP-depleting sodium azide, approximately 50% of the total PTDM uptake remained intact (Figure 6A), indicating a significant contribution from nonenergy dependent uptake pathways, which are likely to include direct translocation.[69,70] When the concentration was increased to 4 μM (Figure 6B), the differences in uptake between standard and ATP-depleted conditions became smaller for all three PTDMs. The homopolymer H_{10} showed an increase in ATP-depleted uptake, the gradient copolymer R_{10} showed the smallest changes, and the block copolymer B_{10} showed a reduction of uptake under standard conditions.

Overall, the changes are relatively minor and these experiments confirm that PTDMs likely have multiple uptake pathways including direct translocation under the experimental conditions studied.[8] The observed variations with concentration are well-known in the PTD literature.[71−76] According to these recent studies, for concentrations below a threshold level, endocytosis is the main pathway for cell entry; at higher concentrations, PTDs enter cells by alternative, energy-independent mechanism. These data suggest the unique distribution of functional groups within the gradient copolymer, compared to its constitutional macromolecular isomers, influences its mode of cellular uptake. Overall, these results showed once more that sequence specific hydrophobicity has an impact on various aspects of PTDM activity and it is an important design parameter to take into consideration.

■ CONCLUSION

Constitutional macromolecular isomeric homopolymers, gradient copolymers, and block copolymers, with the same polymer length and overall composition but increasing hydrophobic segregation, were synthesized and characterized. All of them displayed the ability to induce dye release from mammalian-like lipid vesicles and to be internalized in Jurkat-T cells and HEK293T cells due to the presence of both cationic (guanidine) and hydrophobic (phenyl) components, but they showed different efficiencies, with the homopolymer generally being the most membrane active. The presence of hydrophobic residues within guanidine-rich sequences is known to increase

activity as previously discussed. Here, we have shown, both via biophysical and in vitro cellular assays, that hydrophobic segregation impacts the effectiveness of these PTDMs. This is likely due to the assembly properties of each PTDM, which clearly depend on the spatial distribution of the polar and nonpolar groups. In the case of the block copolymer, the hydrophobic moieties appear to be buried in the micelle core so that only the cationic groups are available for lipid interaction. The membrane activity and internalization efficiency of the gradient copolymer is at least partially explained by its less structured assembly compared to the block copolymer, which exposes both the hydrophobic and cationic components at the surface of the polymer particle to interact with the cell membrane. However, the possibility of alternative explanations to the phenomena is not excluded. All possible explanations, however, can be linked to the sequence specific hydrophobicity of the three PTDMs.

The gradient copolymer was favored over the homopolymer especially in vitro because of its lower cytotoxicity, while retaining higher activity than the block copolymer. However, it is important to note that, although the block copolymer topology was not the most efficient in the specific membrane interactions here examined, its micelle-formation property could be advantageous for cargo delivery purposes, and the effect of linear polymer sequence specific hydrophobicity on the delivery of noncovalently attached cargos is currently under investigation. The role of the norbornene backbone, compared to other polymer backbones like methacrylate and acrylate, is also currently under investigation. We have previously demonstrated the influence side chain spacing plays on activity when comparing polyguanidine-oxanorbornene homopolymers to arginine peptides.[78] Understanding this relationship within polymer backbones would be worthwhile.

■ ASSOCIATED CONTENT

Ⓢ Supporting Information

All detailed experimental procedures and characterizations, including monomer and polymer synthesis, NMR spectra, and GPC traces, as well as the biological assays protocols. This material is available free of charge via the Internet at http://pubs.acs.org.

■ AUTHOR INFORMATION

Corresponding Author

*E-mail: tew@mail.pse.umass.edu.

Notes

The authors declare no competing financial interest.

■ ACKNOWLEDGMENTS

This work was primarily supported by NSF (CHE-0910963). Mass spectral data were obtained at the University of Massachusetts Mass Spectrometry Facility, which is also supported in part by NSF. Michael Lis and Katherine Gibney are acknowledged for assisting with manuscript preparation. Authors also would like to thank Brittany deRonde for contributing to the vesicle data collection and Dr. Gabriela Perez and Prof. Ke Zhang for countless invaluable discussions.

■ REFERENCES

(1) Lin, Y. Z.; Yao, S. Y.; Veach, R. A.; Torgerson, T. R.; Hawiger, J. *J. Biol. Chem.* **1995**, *270*, 14255−14258.
(2) Green, M.; Loewenstein, P. M. *Cell* **1988**, *55*, 1179−1188.
(3) Frankel, A. D.; Pabo, C. O. *Cell* **1988**, *55*, 1189−1193.
(4) Vives, E.; Brodin, P.; Lebleu, B. *J. Biol. Chem.* **1997**, *272*, 16010−16017.
(5) Rothbard, J. B.; Jessop, T. C.; Wender, P. A. *Adv. Drug Delivery Rev.* **2005**, *57*, 495−504.
(6) Mitchell, D. J.; Kim, D. T.; Steinman, L.; Fathman, C. G.; Rothbard, J. B. *J. Pept. Res.* **2000**, *56*, 318−325.
(7) Patel, L. N.; Zaro, J. L.; Shen, W. C. *Pharm. Res.* **2007**, *24*, 1977−1992.
(8) Madani, F.; Lindberg, S.; Langel, U.; Futaki, S.; Graslund, A. *J. Biophys.* **2011**, *2011*, 414729.
(9) Joliot, A.; Pernelle, C.; Deagostinibazin, H.; Prochiantz, A. *Proc. Natl. Acad. Sci. U.S.A.* **1991**, *88*, 1864−1868.
(10) Elmquist, A.; Lindgren, M.; Bartfai, T.; Langel, U. *Exp. Cell Res.* **2001**, *269*, 237−244.
(11) Elliott, G.; OHare, P. *Cell* **1997**, *88*, 223−233.
(12) Futaki, S.; Suzuki, T.; Ohashi, W.; Yagami, T.; Tanaka, S.; Ueda, K.; Sugiura, Y. *J. Biol. Chem.* **2001**, *276*, 5836−5840.
(13) Pooga, M.; Hallbrink, M.; Zorko, M.; Langel, U. *FASEB J.* **1998**, *12*, 67−77.
(14) Futaki, S.; Ohashi, W.; Suzuki, T.; Niwa, M.; Tanaka, S.; Ueda, K.; Harashima, H.; Sugiura, Y. *Bioconjugate Chem.* **2001**, *12*, 1005−1011.
(15) Katayama, S.; Hirose, H.; Takayama, K.; Nakase, I.; Futaki, S. *J. Controlled Release* **2011**, *149*, 29−35.
(16) Rothbard, J. B.; Jessop, T. C.; Lewis, R. S.; Murray, B. A.; Wender, P. A. *J. Am. Chem. Soc.* **2004**, *126*, 9506−9507.
(17) Sakai, N.; Futaki, S.; Matile, S. *Soft Matter* **2006**, *2*, 636−641.
(18) Takeuchi, T.; Kosuge, M.; Tadokoro, A.; Sugiura, Y.; Nishi, M.; Kawata, M.; Sakai, N.; Matile, S.; Futaki, S. *ACS Chem. Biol.* **2006**, *1*, 299−303.
(19) Wimley, W. C.; White, S. H. *Nat. Struct. Mol. Biol.* **1996**, *3*, 842−848.
(20) Sengupta, D.; Smith, J. C.; Ullmann, G. M. *Biochim. Biophys. Acta, Biomembr.* **2008**, *1778*, 2234−2243.
(21) Yau, W. M.; Wimley, W. C.; Gawrisch, K.; White, S. H. *Biochemistry* **1998**, *37*, 14713−14718.
(22) Perret, F.; Nishihara, M.; Takeuchi, T.; Futaki, S.; Lazar, A. N.; Coleman, A. W.; Sakai, N.; Matile, S. *J. Am. Chem. Soc.* **2005**, *127*, 1114−1115.
(23) Witte, K.; Olausson, B. E. S.; Walrant, A.; Alves, I. D.; Vogel, A. *Biochim. Biophys. Acta, Biomembr.* **2013**, *1828*, 824−833.
(24) Walrant, A.; Correia, I.; Jiao, C. Y.; Lequin, O.; Bent, E. H.; Goasdoue, N.; Lacombe, C.; Chassaing, G.; Sagan, S.; Alves, I. D. *Biochim. Biophys. Acta, Biomembr.* **2011**, *1808*, 382−393.
(25) Takayama, K.; Hirose, H.; Tanaka, G.; Pujals, S.; Katayama, S.; Nakase, I.; Futaki, S. *Mol. Pharmaceutics* **2012**, *9*, 1222−1230.
(26) Hennig, A.; Gabriel, G. J.; Tew, G. N.; Matile, S. *J. Am. Chem. Soc.* **2008**, *130*, 10338−10344.
(27) Tezgel, A. O.; Telfer, J. C.; Tew, G. N. *Biomacromolecules* **2011**, *12*, 3078−3083.
(28) Som, A.; Tezgel, A. O.; Gabriel, G. J.; Tew, G. N. *Angew. Chem., Int. Ed.* **2011**, *50*, 6147−6150.
(29) Som, A.; Reuter, A.; Tew, G. N. *Angew. Chem., Int. Ed.* **2012**, *51*, 980−983.
(30) Morris, M. C.; Depollier, J.; Mery, J.; Heitz, F.; Divita, G. *Nat. Biotechnol.* **2001**, *19*, 1173−1176.
(31) Scheller, A.; Oehlke, J.; Wiesner, B.; Dathe, M.; Krause, E.; Beyermann, M.; Melzig, M.; Bienert, M. *J. Pept. Sci.* **1999**, *5*, 185−194.
(32) Oehlke, J.; Lorenz, D.; Wiesner, B.; Bienert, M. *J. Mol. Recogn.* **2005**, *18*, 50−59.
(33) Ziegler, A. *Adv. Drug Delivery Rev.* **2008**, *60*, 580−597.
(34) Elmquist, A.; Hansen, M.; Langel, U. *Biochim. Biophys. Acta, Biomembr.* **2006**, *1758*, 721−729.
(35) Oehlke, J.; Scheller, A.; Wiesner, B.; Krause, E.; Beyermann, M.; Klauschenz, E.; Melzig, M.; Bienert, M. *Biochim. Biophys. Acta, Biomembr.* **1998**, *1414*, 127−139.
(36) Scheller, A.; Wiesner, B.; Melzig, M.; Bienert, M.; Oehlke, J. *Eur. J. Biochem.* **2000**, *267*, 6043−6049.

(37) Tezgel, A. O.; Gonzalez-Perez, G.; Telfer, J. C.; Osborne, B. A.; Minter, L. M.; Tew, G. N. *Mol. Ther.* **2013**, *21*, 201−209.
(38) Kolonko, E. M.; Kiessling, L. L. *J. Am. Chem. Soc.* **2008**, *130*, 5626−5627.
(39) Kolonko, E. M.; Pontrello, J. K.; Mangold, S. L.; Kiessling, L. L. *J. Am. Chem. Soc.* **2009**, *131*, 7327−7333.
(40) Cooley, C. B.; Trantow, B. M.; Nederberg, F.; Kiesewetter, M. K.; Hedrick, J. L.; Waymouth, R. M.; Wender, P. A. *J. Am. Chem. Soc.* **2009**, *131*, 16401−16403.
(41) Geihe, E. I.; Cooley, C. B.; Simon, J. R.; Kiesewetter, M. K.; Edward, J. A.; Hickerson, R. P.; Kaspar, R. L.; Hedrick, J. L.; Waymouth, R. M.; Wender, P. A. *Proc. Natl. Acad. Sci. U.S.A.* **2012**, *109*, 13171−13176.
(42) Bang, E. K.; Gasparini, G.; Molinard, G.; Roux, A.; Sakai, N.; Matile, S. *J. Am. Chem. Soc.* **2013**, *135*, 2088−2091.
(43) Painter, P. C.; Coleman, M. M. *Essentials of Polymer Science and Engineering*; DEStech Publications, Inc.: Lancaster, PA, 2009.
(44) Czerwenka, C.; Polaskova, P.; Lindner, W. *J. Chromatogr. A* **2005**, *1093*, 81−88.
(45) Love, J. A.; Morgan, J. P.; Trnka, T. M.; Grubbs, R. H. *Angew. Chem., Int. Ed.* **2002**, *41*, 4035−4037.
(46) Kiyota, T.; Lee, S.; Sugihara, G. *Biochemistry* **1996**, *35*, 13196−13204.
(47) Lienkamp, K.; Madkour, A. E.; Musante, A.; Nelson, C. F.; Nusslein, K.; Tew, G. N. *J. Am. Chem. Soc.* **2008**, *130*, 9836−9843.
(48) Lambermont-Thijs, H. M. L.; Fijten, M. W. M.; van der Linden, A. J.; van Lankvelt, B. M.; Bloksma, M. M.; Schubert, U. S.; Hoogenboom, R. *Macromolecules* **2011**, *44*, 4320−4325.
(49) Min, K.; Li, M.; Matyjaszewski, K. *J. Polym. Sci., Polym. Chem.* **2005**, *43*, 3616−3622.
(50) Matyjaszewski, K.; Ziegler, M. J.; Arehart, S. V.; Greszta, D.; Pakula, T. *J. Phys. Org. Chem.* **2000**, *13*, 775−786.
(51) Tominaga, Y.; Mizuse, M.; Hashidzume, A.; Morishima, Y.; Sato, T. *J. Phys. Chem. B* **2010**, *114*, 11403−11408.
(52) Kawata, T.; Hashidzume, A.; Sato, T. *Macromolecules* **2007**, *40*, 1174−1180.
(53) Fuchs, S. M.; Raines, R. T. *Biochemistry* **2004**, *43*, 2438−2444.
(54) Yandek, L. E.; Pokorny, A.; Floren, A.; Knoelke, K.; Langel, U.; Almeida, P. F. *Biophys. J.* **2007**, *92*, 2434−2444.
(55) Nishihara, M.; Perret, F.; Takeuchi, T.; Futaki, S.; Lazar, A. N.; Coleman, A. W.; Sakai, N.; Matile, S. *Org. Biomol. Chem.* **2005**, *3*, 1659−1669.
(56) Oda, Y.; Kanaoka, S.; Sato, T.; Aoshima, S.; Kuroda, K. *Biomacromolecules* **2011**, *12*, 3581−3591.
(57) Chen, D. J.; Majors, B. S.; Zelikin, A.; Putnam, D. *J. Controlled Release* **2005**, *103*, 273−283.
(58) Mosmann, T. *J. Immunol. Methods* **1983**, *65*, 55−63.
(59) Zembruski, N. C. L.; Stache, V.; Haefeli, W. E.; Weiss, J. *Anal. Biochem.* **2012**, *429*, 79−81.
(60) Crowley, K. S.; Phillion, D. P.; Woodard, S. S.; Schweitzer, B. A.; Singh, M.; Shabany, H.; Burnette, B.; Hippenmeyer, P.; Heitmeier, M.; Bashkin, J. K. *Bioorg. Med. Chem. Lett.* **2003**, *13*, 1565−1570.
(61) Henriques, S. T.; Costa, J.; Castanho, M. A. R. B. *FEBS Lett.* **2005**, *579*, 4498−4502.
(62) Puckett, C. A.; Barton, J. K. *J. Am. Chem. Soc.* **2009**, *131*, 8738−8739.
(63) Edelson, B. S.; Best, T. P.; Olenyuk, B.; Nickols, N. G.; Doss, R. M.; Foister, S.; Heckel, A.; Dervan, P. B. *Nucleic Acids Res.* **2004**, *32*, 2802−2818.
(64) Fischer, R.; Waizenegger, T.; Kohler, K.; Brock, R. *Biochim. Biophys. Acta, Biomembr.* **2002**, *1564*, 365−374.
(65) Guminski, Y.; Grousseaud, M.; Cugnasse, S.; Brel, V.; Annereau, J. P.; Vispe, S.; Guilbaud, N.; Barret, J. M.; Bailly, C.; Imbert, T. *Bioorg. Med. Chem. Lett.* **2009**, *19*, 2474−2477.
(66) Drin, G.; Cottin, S.; Blanc, E.; Rees, A. R.; Temsamani, J. *J. Biol. Chem.* **2003**, *278*, 31192−31201.
(67) Bergen, J. M.; Kwon, E. J.; Shen, T. W.; Pun, S. H. *Bioconjugate Chem.* **2008**, *19*, 377−384.
(68) Schmid, S. L.; Carter, L. L. *J. Cell Biol.* **1990**, *111*, 2307−2318.
(69) Chae, S. Y.; Kim, H. J.; Lee, M. S.; Jang, Y. L.; Lee, Y.; Lee, S. H.; Lee, K.; Kim, S. H.; Kim, H. T.; Chi, S. C.; Park, T. G.; Jeong, J. H. *Macromol. Biosci.* **2011**, *11*, 1169−1174.
(70) Gros, E.; Deshayes, S.; Morris, M. C.; Aldrian-Herrada, G.; Depollier, J.; Heitz, F.; Divita, G. *Biochim. Biophys. Acta, Biomembr.* **2006**, *1758*, 384−393.
(71) Watkins, C. L.; Schmaljohann, D.; Futaki, S.; Jones, A. T. *Biochem. J.* **2009**, *420*, 179−189.
(72) Kosuge, M.; Takeuchi, T.; Nakase, I.; Jones, A. T.; Futaki, S. *Bioconjugate Chem.* **2008**, *19*, 656−664.
(73) Duchardt, F.; Fotin-Mleczek, M.; Schwarz, H.; Fischer, R.; Brock, R. *Traffic* **2007**, *8*, 848−866.
(74) Wagemans, J. *Biochem. J.* **2007**, *403*, 335−342.
(75) Watkins, C. L.; Brennan, P.; Fegan, C.; Takayama, K.; Nakase, I.; Futaki, S.; Jones, A. T. *J. Controlled Release* **2009**, *140*, 237−244.
(76) Mano, M.; Henriques, A.; Paiva, A.; Prieto, M.; Gavilanes, F.; Simoes, S.; de Lima, M. C. P. *Biochim. Biophys. Acta, Biomembr.* **2006**, *1758*, 336−346.
(77) Braakman, I.; Helenius, J.; Helenius, A. *Nature* **1992**, *356*, 260−262.
(78) Schmidt, N. W.; Lis, M.; Zhao, K.; Lai, G. H.; Alexandrova, A. N.; Tew, G. N.; Wong, G. C. L. *J. Am. Chem. Soc.* **2012**, *134*, 19207−19216.